

Online Learning with Radial Basis Function Networks

Gabriel Borrageiro[✉], Nick Firoozye[✉] and Paolo Barucca[✉]

Abstract—We experiment with the log-returns of financial time series, providing multi-horizon forecasts with a selection of robust supervised learners. We provide two innovative contributions. Firstly, we devise an external input selection algorithm that aims to maximise regression R^2 whilst minimising feature correlations and can operate efficiently in a high-dimensional setting. Secondly, we improve upon the earlier work on radial basis function networks (rbfnets), which applies feature representation transfer from clustering algorithms to supervised learners. Rather than using a randomised, scalar standard deviation for each hidden processing unit (hpu)’s radial basis function, we use a covariance matrix estimated via a Bayesian maximum a posteriori approach. If many training data points are assigned to the j ’th cluster, the j ’th covariance matrix will resemble the maximum likelihood estimate. In contrast, if there are few data points assigned to the j ’th cluster, the j ’th covariance matrix will resemble the diagonalised variance prior. More precisely, we operate with and adapt the precision (inverse covariance) matrices; this leads to a test time fitting time-complexity of $\mathcal{O}(kd^2)$, where k is the number of hpus and d is the external input dimensionality. Our approach leads to a reduction from $\mathcal{O}(kd^3)$ when inverting covariance matrices. Furthermore, we sequentially optimise the hpu parameters with an exponential decay to facilitate regime changes or concept drifts. Our experiments demonstrate that our online rbfnets outperforms a random-walk baseline and several powerful batch learners. The outperformance is not purely down to sequential updating in the test set. Instead, a competitor exponentially weighted recursive least-squares model is updated similarly and performs less well than several batch-learners. Finally, our online rbfnets has hpus that retain greater similarity between training and test vectors, ensuring that it obtains the smallest prediction mean squared errors.

Index Terms—online learning, transfer learning, radial basis function networks, financial time series, multi-step forecasting

I. INTRODUCTION

Financial time series provide several modelling challenges for neural networks and learning systems. These time series are typically both serially correlated and nonstationary. The dynamics of financial assets have been modelled as a jump-diffusion process [1], which is now commonly used in econometrics. The jump-diffusion process implies that financial time series should observe small changes, so-called continuous changes, and occasional jumps over time. One approach for coping with nonstationarity is to learn online continuously. Sequential model fitting may be combined with states-of-nature/transitional learning approaches such as reinforcement learning (rl) or continual learning approaches such

as transfer learning [2]. Sequential learning and prediction models include state-space models such as the Kalman filter [3] and models designed specifically for sequential learning with nonstationary data, such as discounted least-squares [4] and exponentially weighted recursive least squares (ewrls) [5]. Barber et al. [6] consider Bayesian approaches to time series modelling, which are amenable to sequential learning. Transitional learning includes rl, which allows agents to interact with their environment, mapping situations to actions to maximise a numerical award. Well-known temporal-difference algorithms suitable for online learning include q-learning [7] and sarsa [8]. Continual learning is an area of study that asks how artificial systems might learn sequentially, as biological systems do, from a continuous stream of correlated data [9]. They include gradient-based methods [10], [11], meta-learning [12] and transfer learning. Koshiyama et al. [13] apply transfer learning to systematic trading strategy development, with goals of minimising backtest overfitting and generating higher risk-adjusted returns. Borrageiro et al. [14] perform feature representation transfer from radial basis function networks (rbfnets) to sequentially optimised rl agents, who learn to risk-manage and trade currency pairs. Similarly, they apply feature representation transfer from echo state networks to online rl agents who target desired risk positions, earning a funding profit when trading cryptocurrency perpetual swaps [15].

Our paper assesses the benefits of feature selection and online learning with nonlinear models. We limit the scope of our experimentation to financial time series, which at times exhibit high autocorrelation, nonstationarity, nonlinearity and regime-switching characteristics. This behaviour can be classified as concept drift [16]. In section II we introduce the rbfnets and provide a literature review. With section III, we present the Refinitiv cross-asset financial time series data that we use in our experiments. In section IV-A, we discuss the simple yet difficult to beat random-walk baseline. Section IV-B introduces our innovative feature selection meta-algorithm 1 that is used to select minimally correlated, highly predictive external inputs to the various models we use. Section IV-C presents our novel online learning rbfnets. We take the external inputs of feature selection algorithm 1, perform feature representational transfer using k-means++ [17], which determines the rbfnets’ hidden processing units (hpus) as well, and map these hpus to the response using ewrls. The algorithm is compactly described in 2. Section IV-D details a powerful set of competitor models that we compare the performance of the rbfnets against. Section IV-E describes our experiment design, specifically how we use normalised prediction mean squared error (nmse) over multiple forecast horizons to evaluate the performance of our rbfnets and

All authors are affiliated with the Department of Computer Science, University College London, Gower Street, London, WC1E 6BT, United Kingdom. Gabriel Borrageiro is the corresponding author (email: gabriel.borrageiro.20@ucl.ac.uk).

various competitor models against the random-walk baseline. The experiment results are shown in section V.

We find that our online rbfnets obtains the best test set results with minimum nmse. The multi-layer perceptron (mlp) performs worst. If we compare the local learning of the rbfnets with the global learning technique of the mlp, the latter suffers from catastrophic forgetting [11], [18]. The rbfnets that we formulate are naturally designed to measure the similarity between test samples and continuously updated prototypes that capture the characteristics of the feature space. As such, the models are robust in mitigating catastrophic forgetting. In addition, although related to k-nearest neighbours, Gaussian process and kernel ridge regression, our experiments show that the rbfnets, which use clustering algorithms to determine the network's hpus, are more predictive than using each training vector as test-time prototypes. Section VI demonstrates this visually, with plots of the cosine similarity between training vectors and test vectors. The original log-returns space has low similarity whilst the clustered log-returns space has high similarity; thus, more signal is extracted from the data.

II. THE RADIAL BASIS FUNCTION NETWORK

The rbfnets is a single layer network, whose hidden processing units (hpus) are radial basis functions (rbf) of the form

$$\phi_j(\mathbf{x}) = \exp\left(-\frac{1}{2}[\mathbf{x} - \boldsymbol{\mu}_j]^T \boldsymbol{\Sigma}_j^{-1}[\mathbf{x} - \boldsymbol{\mu}_j]\right). \quad (1)$$

The hpu means and covariances are typically learnt through clustering algorithms such as k-means [19]. The hpu outputs are aggregated into a feature vector

$$\boldsymbol{\phi}_t = [1, \phi_1(\mathbf{x}), \dots, \phi_k(\mathbf{x})],$$

and mapped to the response via regression

$$y_t = \boldsymbol{\theta}^T \boldsymbol{\phi}_t + \epsilon.$$

A schematic of the model is shown in figure 1. Figure 2 demonstrates a comparison of several classifiers on synthetic datasets. An mlp separates classes using hpus that form hyperplanes in the input space. The separation of class distributions modelled by local rbfs is probabilistic. The predictive uncertainty increases where there is class-conditional distribution overlap. The rbf activations can be thought of as the posterior feature probabilities, and the weights can be interpreted as the posterior probabilities of class membership, given the presence of the features [20].

Rbfnets have a 'best approximation' property [21]. Essentially, in the set of approximating functions corresponding to all possible choices of parameters, the rbf has minimum approximating error. Seminal papers on rbfnets include [22] and [23]. It is first with [23] that we see the formulation of the rbfnets as a combination of k-means and linear regression. A related, albeit slower method is considered by [24], where they initialise a large rbfnets and rely on orthogonal least squares [25] and forward stepwise selection [26] to select the hpus. They make direct comparisons between the narx model [27] and the rbfnets, demonstrating an application to mimo modelling [28] in simulated dynamic time series. [29] applies a

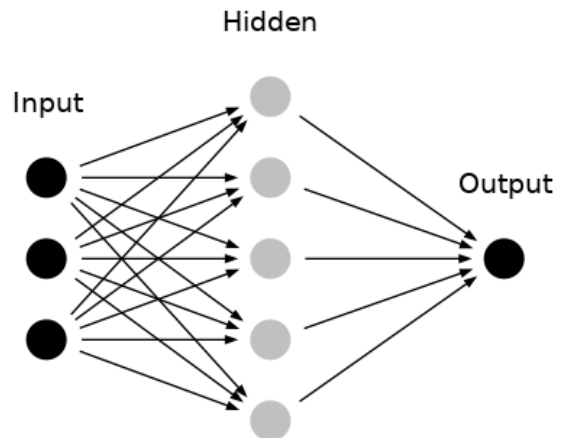


Fig. 1. Architecture of the radial basis function network.

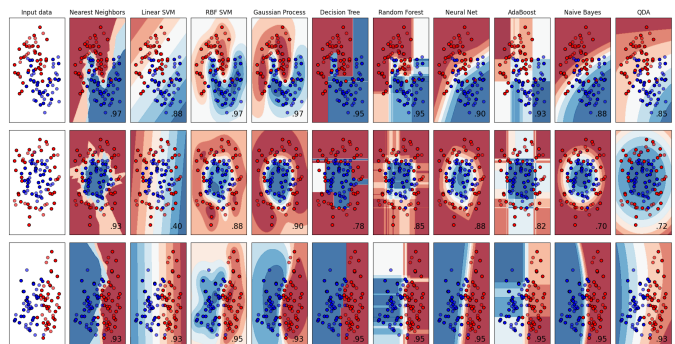


Fig. 2. Comparison of a several scikit-learn classifiers on synthetic datasets.

classical batch-learning rbfnets to macroeconomic forecasting, outperforming benchmarks such as vector autoregression [30] and threshold-var [31] estimators. [32] demonstrates an approach to rbfnets training, which is similar to backpropagation for neural networks [33]. However, he sets some weights between the inputs and hidden layer, rather than the traditional approach, which has weights from the hidden layer to the outputs. He calls this his weighted rbfnets and finds improved accuracy on the UCI letter classification and HODA digit recognition datasets.

The rbfnets relates to the relevance vector machine (rvm) [34], which is a sparse, Bayesian alternative to the support vector machine (svm) [35]. The sparsity is induced by defining an automatic relevance determination Gaussian prior [36], [37] over the model weights. The rvm is a modified version of the Gaussian process regression (gpr) model [38], where the former's hyper-parameters are parameters of the latter's covariance function. However, gpr is more expensive to fit than the rbfnets, with a time-complexity of $\mathcal{O}(n^3)$ and memory complexity of $\mathcal{O}(n^2)$. In contrast, the rbfnets has a time-complexity of $\mathcal{O}(knr)$ for the k-means part, where k is the number of clusters and r is the number of fitting iterations and $\mathcal{O}(n^2k + k^3)$ for the linear regression part. The rbfnets

also relates to k-nearest neighbours (knn) regression [39] as a local learning technique and kernel ridge (k-ridge) regression [40] as a kernel learning method. However, knn, k-ridge and gpr typically use all training examples as prototypes at test time, rendering these techniques less useful for large datasets or nonstationary time series such as financial prices.

III. THE REFINITIV DATASET

Refinitiv is a global financial market data and infrastructure provider. We use their Data Platform Python package to extract daily-sampled data, including currency pairs, equities, rates, credit, metals, commodities, energy and crypto. These are predominately cash instruments but also include futures. The sampled prices are either the last daily traded or quoted limit order book price, with a snapshot taken at 5 pm EST. The dataset begins on 2018-11-01 and ends on 2022-05-20. We reserve half the data for training (649 observations) and the remaining half for testing (648 observations). The full set of constituents, including sector information, is shown in table I.

TABLE I. Experiment constituents, including sector information.

	ric	description	sector
0	BTC=	Bitcoin/US Dollar	crypto
1	ETH=	Ethereum/US Dollar	crypto
2	LTC=	Litecoin/US Dollar	crypto
3	AUD=	Austral. Dollar/US Dollar	fx
4	AUDCHF=	Austral. Dollar/Swiss Franc	fx
5	AUDJPY=	Austral. Dollar/Japanese Yen	fx
6	BRL=	US Dollar/Brazilian Real	fx
7	CAD=	US Dollar/Canadian Dollar	fx
8	CADCHF=	Canadian Dollar/Swiss Franc	fx
9	CADJPY=	Canadian Dollar/Japanese Yen	fx
10	CHF=	US Dollar/Swiss Franc	fx
11	CHFJPY=	Swiss Franc/Japanese Yen	fx
12	CNY=	US Dollar/Chinese Yuan	fx
13	EUR=	Euro/US Dollar	fx
14	EURAUD=	Euro/Austral. Dollar	fx
15	EURCAD=	Euro/Canadian Dollar	fx
16	EURCHF=	Euro/Swiss Franc	fx
17	EURGBP=	Euro/British Pound	fx
18	EURJPY=	Euro/Japanese Yen	fx
19	GBP=	British Pound/US Dollar	fx
20	GBPAUD=	British Pound/Austral. Dollar	fx
21	GBPCAD=	British Pound/Canadian Dollar	fx
22	GBPCHF=	British Pound/Swiss Franc	fx
23	GBPJPY=	British Pound/Japanese Yen	fx
24	GBPNZD=	British Pound/New Zea. Dollar	fx
25	HKD=	US Dollar/Hong Kong Dollar	fx
26	INR=	US Dollar/Indonesia Rupiah	fx
27	JPY=	US Dollar/Japanese Yen	fx
28	KRW=	US Dollar/Korea Won	fx
29	MXN=	US Dollar/Mexico Peso	fx
30	NOK=	US Dollar/Norwegian Krone	fx
31	NZD=	New Zea. Dollar/US Dollar	fx
32	PLN=	US Dollar/Polish Zloty	fx

continued on next page

TABLE I – continued from previous page

	ric	description	sector
33	RUB=	US Dollar/Russian Ruble	fx
34	SEK=	US Dollar/Swedish Krone	fx
35	SGD=	US Dollar/Singapore Dollar	fx
36	TRY=	US Dollar/Turkish Lira	fx
37	TWD=	US Dollar/Taiwanese Dollar	fx
38	ZAR=	US Dollar/South African Rand	fx
39	.BCOM	Bloomberg Commodity	commodities
40	.TRCCRB	Refinitiv CRB	commodities
41	ITEEU5Y=MG	ITRAXX Europe CDS	credit
42	ITEXO5Y=MG	ITRAXX Crossover CDS	credit
43	.TRXFLDGLPUENE	Refinitiv Global Energy	energy
44	.AEX	AEX	equities
45	.AORD	ASX All Ordinaries	equities
46	.AXJO	S&P/ASX 200	equities
47	.BFX	BEL 20	equities
48	.BSESN	S&P Sensex	equities
49	.BVSP	Brazilian IBOVESPA	equities
50	.FCHI	CAC 40	equities
51	.FTAS	FTSE ALL SHARE	equities
52	.FTJ203	JSE All Share	equities
53	.FTSE	FTSE 100	equities
54	.GDAXI	DAX	equities
55	.GSPTSE	TSX Composite	equities
56	.HSI	Hang Seng	equities
57	.IBEX	IBEX 35	equities
58	.IMOEX	MOEX Russia	equities
59	.IRTS	RTS	equities
60	.IXIC	NASDAQ Composite	equities
61	.KLSE	FTSE Bursa KLSE	equities
62	.KS11	Korea Composite	equities
63	.MID	S&P 400 Mid Cap	equities
64	.MXX	Mexican IPC	equities
65	.NDX	NASDAQ 100	equities
66	.NYA	NYSE Composite	equities
67	.OMXHPI	OMX Helsinki	equities
68	.OMXS30	OMX Stockholm 30	equities
69	.SPX	S&P 500	equities
70	.SSEC	Shanghai Composite	equities
71	.SSMI	Swiss Market	equities
72	.STI	Straits Times	equities
73	.STOXX50	EURO STOXX 50	equities
74	.STOXX50E	EURO STOXX 50	equities
75	.TOPX	TOPIX	equities
76	.TRXFLDGLPU	Refinitiv Global Equities	equities
77	.TRXFLDGLPUHLC	Refinitiv Global Healthcare	equities
78	.TRXFLDUSP	Refinitiv United States	equities
79	AU10YT=RR	Australia 10-year Note	rates
80	CA10YT=RR	Canada 10-year Note	rates
81	CH10YT=RR	Swiss 10-year Note	rates
82	CN10YT=RR	China 10-year Note	rates
83	DE10YT=RR	Germany 10-year Note	rates
84	ES10YT=RR	Spain 10-year Note	rates
85	FR10YT=RR	France 10-year Note	rates
86	GB10YT=RR	UK 10-year Note	rates
87	IN10YT=RR	India 10-year Note	rates
88	IT10YT=RR	Italy 10-year Note	rates
89	JP10YT=RR	Japan 10-year Note	rates
90	RU10YT=RR	Russia 10-year Note	rates

continued on next page

TABLE I – concluded from previous page

	ric	description	sector
91	US10YT=RRPS	10-Year Note	rates
92	US2YT=RRPS	2-Year Note	rates
93	US30YT=RRPS	30-Year Bond	rates
94	US5YT=RRPS	5-Year Note	rates
95	ZA10YT=RR	South Africa 10-year Note	rates
96	XAG=	Silver	metals
97	XAU=	Gold	metals
98	XPD=	Palladium	metals
99	XPT=	Platinum	metals

IV. THE RESEARCH EXPERIMENT

We consider the goal of multi-step forecasting with financial time series. Define the prediction mean squared error (mse) for the j 'th model and h 'th forecast horizon as

$$mse_{h,j} = \frac{1}{t-h} \sum_{i=1}^{t-h} (y_{i+h,j} - \hat{y}_{i,j})^2.$$

There are numerous examples in finance where participants seek to minimise mse over optimal horizons h^* that are not known in advance. For example, a market maker captures *edge*, which is half the bid/ask spread, and only realises a profit when the risk is turned over (going from long to short or vice versa) or flattened. This risk turnover is entirely variable. In the context of execution algos, the algo seeks to minimise the implementation shortfall relative to a benchmark. Even if the execution time is known in advance, such as with time-weighted average price algos, the performance of the algo relative to the benchmark is unknown a priori. A final example is systematic proprietary trading strategies, which rely on statistically driven signals to scale in and out of risk over varying time scales. A prediction model that, on average, performs well over multiple forecast horizons is of great value in all the aforementioned cases.

In our experiment which uses the log-returns of the cross-asset Refinitiv dataset introduced in section III, we determine if the rbfnet can provide optimal forecasts over multiple forecast horizons. Optimality is quantified here as the relative performance of the rbfnet to a benchmark, which is the random-walk model. The random-walk model is introduced next, in section IV-A. Our rbfnet differs from earlier work in that its unsupervised and supervised learning components continue to learn in the test set. Specifically, we facilitate online learning for the k-means++ algorithm that learns the network's hpus and maps these hpus to the response using ewrls. A complete algorithm is shown in section IV-C with algorithm 2.

The choice of log-returns is made for several reasons. Firstly, by constructing log-returns, all the time series are considered stationary by unit root tests such as the augmented Dickey-Fuller (adf) test [41]. Secondly, the introduction of log-returns makes the choice of the random-walk as the baseline model most suitable. Finally, we use several comparator models that are discussed in section IV-D, that rely on the independent and identically distributed (iid) random variables assumption. These competitors are traditional batch-learning models and cannot be fitted practically sequentially in several cases. For example, the gradient tree boosters and random forests use underlying trees that are grown using the cart algorithm [42]. For regression trees, the cart algorithm will

split the training set by feature indices and values as necessary to reduce the total mse in the tree. Therefore, it is not computationally feasible to apply the algorithm at test time to the original training dataset augmented by new test entries. In addition, some of the models use an L-BFGS solver [43] for parameter optimisation, which is purely a batch method. Aside from this, to demonstrate that the results we get with the rbfnet are not purely down to sequential optimisation in the test set, we use a second online learning model, the ewrls.

A. The Random-Walk Model

The random-walk model [44]

$$y_t = y_{t-1} + \epsilon_t,$$

has stationary expectation

$$\mathbb{E}[y_t] = y_0,$$

yet nonstationary variance and covariance

$$Var[y_t] = t\sigma^2$$

$$Cov[y_t, y_{t-\tau}] = |t - \tau|\sigma^2.$$

A large body of academic literature shows that it is difficult to beat the random-walk model when forecasting returns of financial time series [45], [46]. [47] considers price series as Gaussian random walks, whose increments are iid Gaussian random variables. Bachelier's first law states that the variation of returns grows with the square root of time. [48] find that Bachelier's first law holds well for actual financial returns; however, they also find that standard Gaussian random-walk models for financial returns modelling underestimate the extreme fluctuations that are empirically observed. Furthermore, they find that price changes follow fat-tailed, power-law distributions, with extreme events not as rare as Gaussian models might predict. Finally, they find that market activity and volatility are highly intermittent in time, with intense activity intertwined with periods of calm; these are the behavioural characteristics modelled by the jump-diffusion hypothesis.

B. Feature Selection

In our experiment, we have one hundred assets to choose from as external inputs to the models we use. There is much redundancy in this external input space. For example, figure 3 shows the training set log-return correlations visually, with an overwhelming red colour indicating positive correlation. Furthermore, table II shows the distribution of the off-diagonal correlation values, which averages just under 6% and has a maximum value of almost 100%. Correlated features are likely to result in more significant prediction variance. Denote the singular value decomposition [49] of the training set features as

$$\mathbf{X} = \mathbf{USV}^T,$$

where \mathbf{S} is the diagonal matrix of eigenvalues. The variance of the least-squares parameters is:

$$Var[\boldsymbol{\theta}] = \sigma^2(\mathbf{X}^T\mathbf{X})^{-1} = \sigma^2\mathbf{VS}^{-2}\mathbf{V}^T.$$

TABLE II
TRAINING SET LOG-RETURN CORRELATION DISTRIBUTION.

	count	mean	std	min	25%	50%	75%	max
ρ	9900	0.056	0.276	-0.82	-0.12	0.018	0.221	0.996

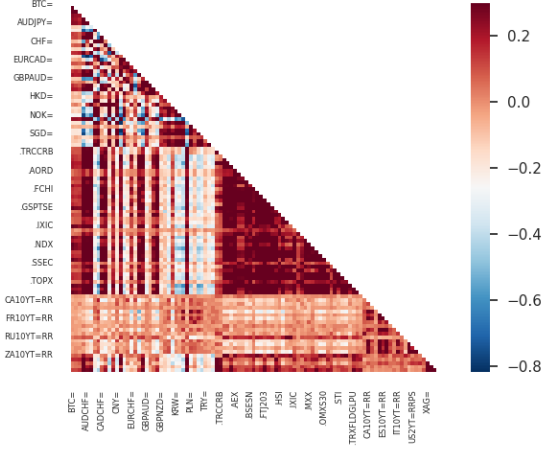


Fig. 3. Training set log-return correlations.

Highly correlated features in \mathbf{X} cause \mathbf{S}^{-2} to be large, which increases $\text{Var}[\theta]$.

There are various feature selection algorithms such as forward stepwise, backward stepwise, forward stagewise and lasso, which Hastie et al. [50] discuss in detail. Forward stepwise scales well as the dimensionality d of the feature space $\mathbf{X} \in \mathbb{R}^{n \times d}$ increases. However, forward stepwise selection works on the principle of selecting features that maximise R^2 or minimise mse without considering the correlation between the features themselves. On the other hand, variance inflation factor (vif) minimisation [51] does concern itself with feature selection based on minimising the correlation between features. Nevertheless, vif minimisation does not care if the selected features result in high R^2 relative to the response. Therefore, in algorithm 1, we novelly combine forward stepwise selection and vif minimisation to the training set log-returns. The algorithm is applied to each target, and the target-conditional subset of external inputs is held fixed during test set evaluation. An example of the algorithm's output (to two decimal places) is shown in table III. The target is the training set one-step-ahead daily returns of the EURUSD currency pair. We see that the $R^2 = 0.15$, with the features ranked in order of their contribution to total R^2 . Other statistics shown are the regression parameter t-values, which are the estimated regression coefficients divided by their standard errors. The associated p-values can be compared against the 5% critical value and standard frequentist statistics hypotheses of statistical significance inferred. Other statistics included are the normalised mse (nmse) which is the regression mse divided by the variance of the response, which shows predictive quality in that the nmse is less than 1. Furthermore, the Durbin-Watson (dw) statistic [52] for serial autocorrelation is around

2, indicating no serial correlation in the regression residuals. Finally, the adf statistic shows that the regression residuals are stationary.

Algorithm 1: Forward stepwise selection with variance inflation factor minimisation.

Require: κ // the maximum vif

Initialise: $\mathbb{S} = [1, 2, \dots, d]$, $\mathbf{r} = \mathbf{v} = \mathbf{0} \in \mathbb{R}^d$

Input: \mathbf{X}, \mathbf{y}

Output: $\mathbb{S} \in \mathbb{Z}^p$, $0 < p \leq d$

```

1 for  $j \leftarrow 1$  to  $d$  do
2    $\bar{\mathbf{y}} = \frac{1}{n} \sum_{i=1}^n \mathbf{y}_i$ 
3    $\bar{\mathbf{x}}_j = \frac{1}{n} \sum_{i=1}^n \mathbf{X}_{ij}$ 
4    $\theta_j = \frac{\sum_{i=1}^n (\mathbf{y}_i - \bar{\mathbf{y}})(\mathbf{X}_{ij} - \bar{\mathbf{x}}_j)}{\sum_{i=1}^n (\mathbf{X}_{ij} - \bar{\mathbf{x}}_j)^2}$ 
   //  $\mathbf{r}_j$  is the  $R^2$  of a regression of  $\mathbf{y}$  on  $\mathbf{x}_j$ .
5    $\mathbf{r}_j = R_{\mathbf{y}|\mathbf{x}_j}^2 = 1 - \frac{\sum_{i=1}^n (\mathbf{y}_i - \theta_j \mathbf{X}_{ij})^2}{\sum_{i=1}^n (\mathbf{y}_i - \bar{\mathbf{y}})^2}$ 
   //  $R_{\mathbf{x}_j|\mathbf{x}_{-j}}^2$  denotes the  $R^2$  of a regression of
   //  $\mathbf{x}_j$  onto the remaining predictors,
   // excluding the  $j$ 'th one.
6    $\mathbf{v}_j = \frac{1}{1 - R_{\mathbf{x}_j|\mathbf{x}_{-j}}^2}$ 
7 end
8 Sort  $\mathbf{r}$  in ascending order and use the index to sort  $\mathbb{S}$ .
9 while  $\forall \mathbf{v} \geq \kappa$  do
10  for  $j \leftarrow 1$  to  $d$  do
11    if  $\mathbf{v}_j \geq \kappa$  then
12      remove  $\mathbb{S}_j$ 
13      recompute  $\mathbf{v}$ 
14    end
15  end
16 end
```

C. The Online Learning Radial Basis Function Network

Algorithm 2 shows our online learning rfbnet. In the training set, the algorithm resembles the standard algorithm of [23], relying on k-means++ to learn the hpu means, then finally mapping the hpu output to the response using ridge regression. An innovation that we make relative to the earlier work is that whilst the earlier work uses a randomised, scalar standard deviation σ_j in the rbf equation 1, we apply a Bayesian maximum a posteriori (map) estimate to the covariance matrices that we use instead. If many training data points are assigned to the j 'th cluster, the j 'th covariance matrix will resemble the maximum likelihood estimate. In contrast, if there are few data points assigned to the j 'th cluster, the j 'th covariance matrix will resemble the diagonalised variance prior. A further innovation we make is the online updating of the hpu means and covariances, with exponential decay to allow for regime changes or concept drifts [16]. We operate with and adapt the precision (inverse covariance) matrices more precisely; this leads to a test time time-complexity of $\mathcal{O}(kd^2)$, a reduction from $\mathcal{O}(kd^3)$ when operating on covariance matrices. Finally, we use ewrls to map the hpu outputs to the response. Ewrls operates efficiently with a precision matrix of the hpu space. Note that ewrls updating can show instabilities, especially if the exponential half-life is $\tau < 0.95$. In this case, a variance

TABLE III

FORWARD STEPWISE SELECTION AND VIF MINIMISATION APPLIED TO THE EURUSD SPOT FX RETURNS IN THE TRAINING SET.

	value	t-value	crit-value	p-value	vif	R^2
EUR=						
R^2	0.15					
n	648					
σ^2	0.00					
mse	0.00					
nmse	0.79					
dw	2.02		0.05	0.02		
adf	-25.7		-2.9	0.00		
NOK=	-0.08	-2.18	0.05	0.01	4.62	0.012
.MID	0.04	2.80	0.05	0.00	4.29	0.011
CAD=	-0.09	-1.69	0.05	0.04	2.43	0.010
ITEXO5Y=MG	0.01	0.26	0.05	0.39	4.04	0.009
.FTJ203	0.01	0.77	0.05	0.22	3.46	0.009
NZD=	-0.01	-0.23	0.05	0.40	2.75	0.008
.BSESN	0.03	1.86	0.05	0.03	2.26	0.008
.BVSP	-0.01	-0.76	0.05	0.22	3.07	0.007
XPD=	0.01	1.24	0.05	0.10	1.94	0.006
SEK=	0.02	0.50	0.05	0.30	3.59	0.006
.MXX	0.01	0.68	0.05	0.24	2.12	0.005
PLN=	-0.02	-0.55	0.05	0.28	3.11	0.005
MXN=	0.03	1.06	0.05	0.14	3.12	0.005
XPT=	-0.00	-0.49	0.05	0.30	2.60	0.004
GBP=	-0.00	-0.25	0.05	0.40	2.01	0.004
.TRCCRB	-0.01	-0.86	0.05	0.19	2.03	0.003
.AXJO	-0.00	-0.50	0.05	0.30	2.06	0.003
BTC=	0.01	1.99	0.05	0.02	2.95	0.003
XAG=	-0.01	-0.77	0.05	0.22	3.61	0.003
RU10YT=RR	-0.03	-1.04	0.05	0.14	1.56	0.003
CHFJPY=	0.08	1.90	0.05	0.02	1.55	0.003
BRL=	-0.04	-2.14	0.05	0.01	1.75	0.002
.STI	-0.02	-0.95	0.05	0.16	2.96	0.002
XAU=	0.03	1.30	0.05	0.09	3.26	0.002
ETH=	0.00	0.32	0.05	0.37	3.38	0.002
IT10YT=RR	-0.01	-0.73	0.05	0.23	1.80	0.002
IN10YT=RR	0.09	2.41	0.05	0.00	1.22	0.002
ES10YT=RR	0.02	0.59	0.05	0.27	2.02	0.002
.KLSE	0.02	0.83	0.05	0.20	2.27	0.002

stabilisation update can be applied after line 19 of algorithm 2, which is essentially $\mathbf{P}_t = \mathbf{P}_t \tau$. Regularisation of ewrls is discussed by [53]. Furthermore, regression regularisation approaches suitable for online learning with nonstationary data are studied by [54].

D. Competitor Models

The models we consider in our experiment are shown next. We use scikit-learn [55] implementations for Gaussian process regression, gradient tree boosting, k-nearest neighbours regression, the multi-layer perceptron, the random forest and support vector regression. We use our implementations of ridge regression, kernel ridge regression, ewrls and the rbfnet. The online rbfnet faces a robust assortment of competitor models, which in most cases are suited to or can only be fitted by batch learning.

- **random-walk** - this is the baseline model that is discussed in section IV-A.
- **gpr** - the Gaussian process regression model [56]. We combine an rbf kernel with a white noise kernel. Scikit-learn uses an L-BFGS solver by default.

Algorithm 2: The online learning radial basis function network.

Require: k // the number of hpus
 α // the ridge penalty
 $0 \ll \tau < 1$ // an exponential forgetting factor
Initialise: $v_0 = d + 2$, $\boldsymbol{\theta} = \mathbf{0} \in \mathbb{R}^{k+1}$, $\mathbf{P} = \mathbf{I}_{k+1}/\alpha$
Hpu parameterisation via k-means++:
 // This section uses the training set feature matrix $\mathbf{X} \in \mathbb{R}^{n \times d} = \{\mathbf{x}_i^T\}_{i=1}^n$

- 1 Initialise the hpu means $\{\boldsymbol{\mu}_j\}_{j=1}^k$.
- 2 **repeat**
- 3 Assign the feature training vector to the nearest hpu mean, $\delta_{j,i} = \arg \min_j \|\mathbf{x}_i - \boldsymbol{\mu}_j\|_2^2$.
 // $\delta_{j,i} = 1$ and $\delta_{k,i} = 0 \quad \forall k \neq j$
- 4 Update each hpu mean using all the points assigned to it, $\boldsymbol{\mu}_j = \frac{1}{n_j} \sum_{i=1}^n \delta_{j,i} \mathbf{x}_i$.
- 5 **until until convergence;**
 // Learn the hpu covariances via Bayesian MAP estimation
- 6 Estimate the prior scatter matrix $\mathbf{S}_0 = \frac{1}{k^{1/d}} \text{diag}(s_1^2, \dots, s_d^2)$ where $s_j = (1/n) \sum_{i=1}^n (x_i - \bar{x}_j)^2$.
- 7 Estimate the j 'th likelihood scatter matrix $\mathbf{S}_j = \sum_{i=1}^n \delta_{j,i} (\mathbf{x}_i - \bar{\mathbf{x}}_j)(\mathbf{x}_i - \bar{\mathbf{x}}_j)^T$.
- 8 The j 'th posterior covariance is $\boldsymbol{\Sigma}_j = \frac{\mathbf{S}_0 + \mathbf{S}_j}{v_0 + n_j + d + 2}$, where $n_j = \sum_i \delta_{j,i}$.
- 9 The j 'th precision matrix is $\boldsymbol{\Lambda}_j = \boldsymbol{\Sigma}_j^{-1}$.

Output: \hat{y}_t
 // This is the online update, with test-time data $\{\mathbf{x}_t \in \mathbb{R}^d, y_t\}$.

- 10 $\delta_{j,t} = \arg \min_j \|\mathbf{x}_t - \boldsymbol{\mu}_j\|_2^2$
- 11 $\boldsymbol{\mu}_{j,t} = \tau \boldsymbol{\mu}_{j,t-1} + (1 - \tau) \mathbf{x}_t$
- 12 $a_t = 1 + (\mathbf{x}_t - \boldsymbol{\mu}_{j,t})^T \boldsymbol{\Lambda}_{j,t-1} (\mathbf{x}_t - \boldsymbol{\mu}_{j,t}) / \tau$
- 13 $\mathbf{k}_t = \boldsymbol{\Lambda}_{j,t-1} (\mathbf{x}_t - \boldsymbol{\mu}_{j,t}) / (\tau a_t)$
- 14 $\boldsymbol{\Lambda}_{j,t} = \boldsymbol{\Lambda}_{j,t-1} / \tau - \mathbf{k}_t \mathbf{k}_t^T a_t$
 // Map the hpus to the response using ewrls.
- 15 $\phi_h(\mathbf{x}_t) = \exp\left(-\frac{1}{2} [\mathbf{x}_t - \boldsymbol{\mu}_{h,t}]^T \boldsymbol{\Lambda}_{j,t} [\mathbf{x}_t - \boldsymbol{\mu}_{h,t}]\right), \quad \forall h = 1, \dots, k$
- 16 $\boldsymbol{\phi}_t = [1, \phi_1(\mathbf{x}_t), \dots, \phi_k(\mathbf{x}_t)]^T$
- 17 $b_t = 1 + \boldsymbol{\phi}_{t-1}^T \mathbf{P}_{t-1} \boldsymbol{\phi}_{t-1} / \tau$
- 18 $\mathbf{m}_t = \mathbf{P}_{t-1} \boldsymbol{\phi}_{t-1} / (b_t \tau)$
- 19 $\boldsymbol{\theta}_t = \boldsymbol{\theta}_{t-1} + \mathbf{m}_t (y_t - \boldsymbol{\theta}_{t-1}^T \boldsymbol{\phi}_{t-1})$
- 20 $\mathbf{P}_t = \mathbf{P}_{t-1} / \tau - \mathbf{m}_t \mathbf{m}_t^T b_t$
- 21 $\hat{y}_t = \boldsymbol{\theta}_t^T \boldsymbol{\phi}_t$

- **gtb** - the gradient tree boosting regression model [57], with a default one hundred estimators, a maximum tree depth of 3 and the mse splitting criteria.
- **k-ridge** - kernel ridge regression [40].
- **knn** - k-nearest neighbours regression [39], with a default 5 nearest neighbours and Minkowski distance metric [58]. The scikit-learn implementation automatically decides between ball-tree and kd-tree algorithms [59] to compute the nearest neighbors.
- **mlp** - multi-layer perceptron regression [60]. Note that we use the L-BFGS solver, which converges faster and with better solutions on small datasets. We use the default

structure of a single layer comprised of one hundred hpus that use the relu activation.

- **rf** - random forests of regression trees [61], with a default one hundred estimators. Each tree in the forest is grown to an unrestricted depth and pruned back using minimal cost complexity pruning [42].
- **ridge** - the ridge regression model [62].
- **svm** - the support vector regression model, specifically the ν -svr, where ν controls the number of support vectors [63], [64]. This scikit-learn implementation uses the rbf kernel by default.
- **ewrls** - exponentially weighted recursive least-squares, discussed in section IV-C.
- **rbfnet** - the online learning radial basis function network detailed in algorithm 2. We set $k = 100$ hpus.

E. Experiment Design

As discussed in section III, we construct daily log-returns and set half the data aside for training and the other half for testing. We apply the external input selection algorithm 1 to the training set log-returns and end up with a subset of external inputs per target. These are held fixed and used as is in the test set. We set the maximum vif $\kappa = 5$. For the various models that use ridge penalties, we use a default value of $\alpha = 0.0001$. Both the ewrls and rbfnets use an exponential decay factor $\tau = 0.99$. During test time, these two models continue to be fitted online. The performance criteria that we consider is normalised prediction mean squared error (nmse) for forecast horizons in days $h = 1, \dots, 30$

$$nmse_{h,j} = \frac{\sum_{i=1}^{t-h} (y_{i+h,j} - \hat{y}_{i,j})^2}{\sum_{i=1}^{t-h} (y_{i+h,j} - y_{0,j})^2}. \quad (2)$$

In equation 2, the normalisation of mse occurs relative to the random-walk baseline. We consider a second performance measure that is less important than nmse in a financial time series forecasting context: the forecast accuracy is defined as

$$acc_{h,j} = \frac{1}{t-h} \sum_{i=1}^{t-h} I[\text{sign}(y_{i+h,j}) = \text{sign}(\hat{y}_{i,j})],$$

where $I[\cdot]$ is an indicator function that returns 1 for a true condition, or else 0, and

$$\text{sign}(x) = \begin{cases} 1 & \text{if } x > 0 \\ 0 & \text{if } x = 0 \\ -1 & \text{if } x < 0 \end{cases}.$$

V. RESULTS

Table IV shows that several models have average test set nmse that is better than the random-walk baseline. These include ewrls, gpr, gtb, k-ridge, rbfnet and rf. The models that perform worse than the random-walk baseline include knn, mlp, ridge and svm, with the mlp the worst performing model. The rbfnet has the lowest average nmse of 0.636. Comparing this to the second-best result, a nmse of 0.673 for gpr, we perform a two-sample t-test for equal means [65] and find that the means are considered statistically different, drawn from

differently parameterised distributions. For all models, we also perform a Wald test [66] for the null hypothesis that the nmse is no different from 1, tested at the 5% critical value. We find that in all cases, the model-averaged nmse is statistically different from 1. Figure 4 shows the nmse by model and forecast horizon. There is a similar performance between the rbfnet and gpr for $h = 1$. For $h = 2, \dots, 30$, the rbfnet outperforms gpr, the random-walk baseline and the remaining competitor models. We cannot put the rbfnet outperformance down to sequential updating alone in the test set; if this were the case, the ewrls model would outperform the remaining offline learning models. Instead, ewrls performs worse than gpr, rf, gtb and k-ridge, which are all offline learning models. Finally, table V shows forecast accuracy by model for the horizons $h = 1, \dots, 30$. The gtb has the highest accuracy at 83.1%, followed by gpr at 82.7%. Rf, k-ridge and the rbfnet follow closely behind. The worst performing model is ridge regression, with 54.7% accuracy. Nevertheless, a two-sample t-test for equal means, where the comparison is made between the mlp accuracy and a Bernoulli distributed mean of 50% with a variance of 0.25%, concludes that the ridge model has statistically better accuracy than pure chance.

TABLE IV
TEST SET NMSE BY MODEL.

model	ewrls	gpr	gtb	k- ridge	knn	mlp	rbfnet	rf	ridge	svm
targets	100	100	100	100	100	100	100	100	100	100
count	3000	3000	3000	3000	3000	3000	3000	3000	3000	3000
mean	0.976	0.673	0.781	0.797	1.068	2.709	0.636	0.763	1.221	1.197
std	0.523	0.561	0.894	0.929	0.914	4.188	0.415	0.821	0.843	1.613
min	0.266	0.037	0.041	0.039	0.134	0.081	0.141	0.035	0.476	0.123
25%	0.608	0.315	0.312	0.302	0.423	0.712	0.360	0.322	0.830	0.434
50%	0.855	0.482	0.507	0.547	0.809	1.314	0.514	0.499	1.020	0.682
75%	1.146	0.845	0.900	0.869	1.327	3.064	0.795	0.868	1.359	1.190
max	3.395	3.374	5.703	5.338	5.006	25.7	2.46	5.734	8.332	11.9
se	0.010	0.010	0.016	0.017	0.017	0.076	0.008	0.015	0.015	0.029
t-value	-	-	-	-	4.06	22.3	-	-	14.3	6.70
	2.49	31.9	13.4	11.9			48.1	15.8		
crit-value	0.05	0.05	0.05	0.05	0.05	0.05	0.05	0.05	0.05	0.05
p-value	0.006	0.000	0.000	0.000	0.000	0.000	0.000	0.000	0.000	0.000
reject H_0 :	1	1	1	1	1	1	1	1	1	1
$\mu = 1$										

TABLE V
TEST SET ACCURACY BY MODEL.

model	ewrls	gpr	gtb	k- ridge	knn	mlp	rbfnet	rf	ridge	svm
targets	100	100	100	100	100	100	100	100	100	100
count	3000	3000	3000	3000	3000	3000	3000	3000	3000	3000
mean	0.625	0.827	0.831	0.815	0.698	0.596	0.809	0.825	0.547	0.771
std	0.303	0.191	0.190	0.191	0.287	0.298	0.163	0.194	0.374	0.222
min	0.000	0.076	0.047	0.187	0.002	0.002	0.106	0.011	0.000	0.063
25%	0.432	0.777	0.812	0.763	0.532	0.313	0.749	0.783	0.134	0.664
50%	0.746	0.902	0.903	0.897	0.797	0.681	0.852	0.900	0.691	0.855
75%	0.883	0.947	0.944	0.940	0.937	0.870	0.908	0.943	0.928	0.937
max	0.980	0.997	0.997	0.998	0.991	0.989	1.000	0.998	0.998	1.000

VI. DISCUSSION

Our rbfnets apply sequentially adapted feature representation transfer from clustering algorithms to supervised learners.

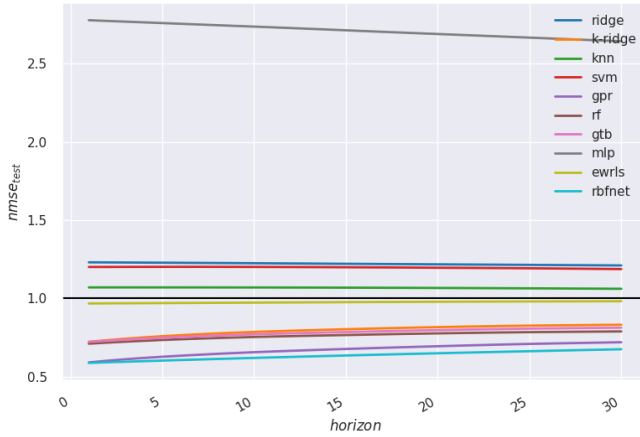


Fig. 4. Test set nmse by model and forecast horizon in days.

Online transfer learning is a relevant area of research for non-stationary time series. Although transfer learning is primarily concerned with transferring knowledge from a source domain to a target domain and may be used in an offline or online setting, an increasing number of papers focus on online transfer learning [67]–[69]. Our paper contributes to the research of continual learning in financial time series by demonstrating that continual learning benefits multi-step forecasting, above and beyond sequential learning. If we compare the local learning of the rbfnet with the global learning technique of the feed-forward neural network, the latter suffers from catastrophic forgetting. Kirkpatrick et al. [11] and Sukhov et al. [18] look at ways of improving this issue, specifically at training networks that can maintain expertise on tasks that they have not experienced for a long time. The rbfnets that we formulate are naturally designed to measure the similarity between test samples and continuously updated prototypes that capture the characteristics of the feature space. As such, the models are robust in mitigating catastrophic forgetting. To demonstrate this, we conduct a small experiment that measures the cosine similarity

$$\text{cosine similarity} = \frac{\mathbf{a} \cdot \mathbf{b}}{\|\mathbf{a}\| \|\mathbf{b}\|},$$

between training and test vectors of the financial assets used in the main research experiment. The range of this function is between -1 (complete dissimilarity) and 1 (total similarity). Similar to correlation, a value of 0 indicates no similarity. Using the previous train/test split, we measure the cosine similarity between the training set log-returns with itself and with the test set log-returns. Figure 5 and table VI indicates that the log-returns have cosine similarity close to zero, and the similarity approaches 0 as the distance in time between the training and test set vectors increases; this is despite the stationary and iid nature of the log-returns. Figure 5 and table VI also shows the cosine similarity between the training and test set hpu outputs. We observe regions of high similarity, interspersed with periods of low similarity. For example, a substantial period of low similarity occurs in March 2020,

when risky assets such as equities, crypto and commodities sold off massively on the back of global economic shutdowns induced by Covid-19. The hpu cosine similarities average 38% when comparing train versus train vectors and degrade a fraction when comparing train versus test vectors, averaging 35.7%. Perhaps it is unsurprising that the rbfnet hpu means and covariances retain greater signal in the input feature space. The regime-switching models of [70] rely on Gaussian mixture models (gmms) to capture the regime-switching characteristics of economic time series. K-means can be thought of as a variant of expectation-maximisation [71] which is used to perform maximum likelihood estimates for gmms. By comparing the similarity plots of the original feature space on the left and the clustered feature space on the right, we see the differences between models such as k-ridge and the rbfnet. The k-ridge model will pull the test vectors toward training prototypes that may say little about forecast capability for hitherto unseen data. In contrast, the rbfnets measure the similarity of test vectors with hpus that have learned the feature space’s intrinsic nature.

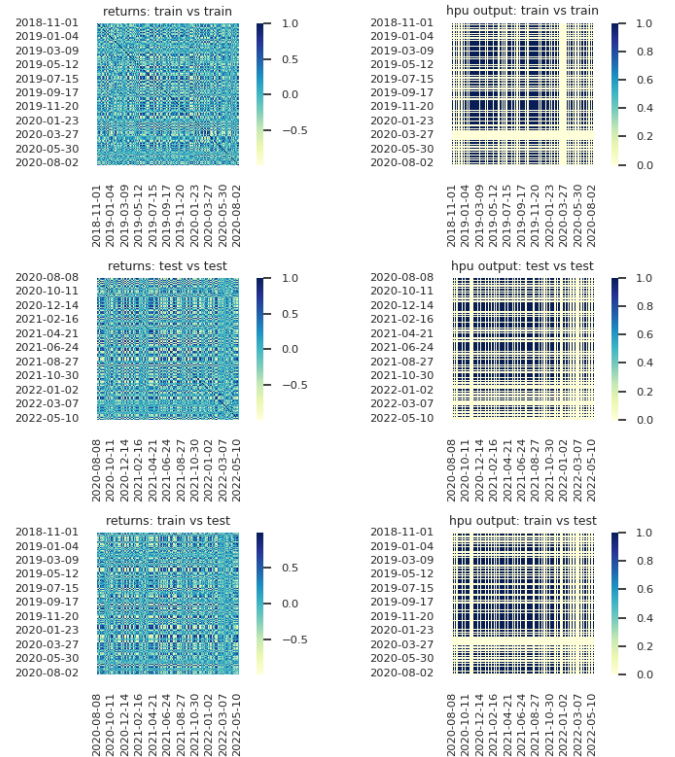


Fig. 5. Returns and hidden processing unit (hpu) cosine similarities.

VII. CONCLUSION

Financial time series exhibit the attributes of autocorrelation, nonstationarity and nonlinearity. Our experiment demonstrates the added value of feature selection, nonlinear modelling, and online learning when providing multi-horizon forecasts. Technically, by constructing log-returns, the time series become stationary as measured by unit root tests; therefore, offline batch learning is possible. However, we find experimental

TABLE VI
RETURNS AND HIDDEN PROCESSING UNIT (HPU) COSINE SIMILARITIES.

	mean	std
log-returns: train vs train	0.004	0.373
log-returns: test vs test	0.005	0.415
log-returns: train vs test	0.002	0.385
hpu output: train vs train	0.381	0.486
hpu output: test vs test	0.335	0.472
hpu output: train vs test	0.357	0.479

evidence to support the use of online, nonlinear learning via feature representational transfer learning rbfnet. The rbfnet obtain the best experiment results, which can be attributed primarily to the clustering algorithms they use, which learn the intrinsic nature of the feature space; the resulting hpus provide predictive prototypes for unseen test data, which retain high similarity across time.

REFERENCES

- [1] R. C. Merton, "Option pricing when underlying stock returns are discontinuous," *Journal of Financial Economics*, vol. 3, no. 1, pp. 125–144, 1976.
- [2] Q. Yang, Y. Zhang, W. Dai, and S. J. Pan, *Transfer Learning*. Cambridge University Press, 2020.
- [3] R. E. Kalman, "A new approach to linear filtering and prediction problems," *Journal of Basic Engineering*, vol. 82, no. 1, p. 35, 1960.
- [4] B. Abraham and J. Ledolter, *Statistical methods for forecasting*. Wiley, 1983.
- [5] W. Liu, J. C. Principe, and S. Haykin, *Kernel Adaptive Filtering: A Comprehensive Introduction*, 1st ed. Wiley Publishing, 2010.
- [6] D. Barber, C. Taylan, and C. Silvia, *Bayesian Time Series Models*. Cambridge University Press, 2011.
- [7] C. J. Watkins, "Learning from delayed rewards," Ph.D. dissertation, King's College, Oxford, 1989.
- [8] G. A. Rummery and M. Niranjan, "On-line q-learning using connectionist systems," in *Technical Report CUED/F-INFENG/TR 166, Cambridge University Engineering Department*, 1994.
- [9] R. Hadsell, D. Rao, A. Rusu, and R. Pascanu, "Embracing change: Continual learning in deep neural networks," *Trends in cognitive sciences*, vol. 24, pp. 1028–1040, 2020.
- [10] C. Kaplanis, M. Shanahan, and C. Clopath, "Continual reinforcement learning with complex synapses," 2018.
- [11] J. Kirkpatrick, R. Pascanu, N. Rabinowitz, J. Veness, G. Desjardins, A. Rusu, K. Milan, J. Quan, T. Ramalho, A. Grabska-Barwinska, D. Hassabis, C. Clopath, D. Kumaran, and R. Hadsell, "Overcoming catastrophic forgetting in neural networks," *Proceedings of the National Academy of Sciences of the United States of America*, vol. 114, pp. 3521–3526, 2017.
- [12] J. X. Wang, Z. Kurth-Nelson, D. Tirumala, H. Soyer, J. Z. Leibo, R. Munos, C. Blundell, D. Kumaran, and M. Botvinick, "Learning to reinforcement learn," 2017.
- [13] A. Koshiyama, S. B. Blumberg, S. Flennerhag, N. Firoozye, and P. Treleven, "Quantnet: Transferring learning across systematic trading strategies," 2020.
- [14] G. Borraigeiro, N. Firoozye, and P. Barucca, "Reinforcement learning for systematic fx trading," *IEEE Access*, vol. 10, pp. 5024–5036, 2022.
- [15] —, "The recurrent reinforcement learning crypto agent," *IEEE Access*, pp. 1–1, 2022.
- [16] A. S. Iwashita and J. P. Papa, "An overview on concept drift learning," *IEEE access*, vol. 7, pp. 1532–1547, 2019.
- [17] D. Arthur and S. Vassilvitskii, "K-means++: The advantages of careful seeding," in *Proceedings of the Eighteenth Annual ACM-SIAM Symposium on Discrete Algorithms*, ser. SODA '07. USA: Society for Industrial and Applied Mathematics, 2007, p. 1027–1035.
- [18] S. Sukhov, M. Leontev, A. Miheev, and K. Sviatov, "Prevention of catastrophic interference and imposing active forgetting with generative methods," *Neurocomputing (Amsterdam)*, vol. 400, pp. 73–85, 2020.
- [19] S. Lloyd, "Least squares quantization in pcm," *IEEE transactions on information theory*, vol. 28, no. 2, pp. 129–137, 1982.
- [20] C. M. Bishop, *Neural networks for pattern recognition*. Oxford University Press, 1995.
- [21] F. Girosi and T. Poggio, "Networks and the best approximation property," *Biological cybernetics*, vol. 63, no. 3, pp. 169–176, 1990.
- [22] D. Broomhead and D. Lowe, "Multivariable functional interpolation and adaptive networks," *Complex Syst.*, vol. 2, 1988.
- [23] J. Moody and C. J. Darken, "Fast learning in networks of locally-tuned processing units," *Neural computation*, vol. 1, pp. 281–294, 1989.
- [24] S. A. Billings, C. F. Fung, and W. Luo, *On-Line Supervised Adaptive Training Using Radial Basis Function Networks*. Department of Automatic Control and Systems Engineering, 1996.
- [25] I. Markovskiy and S. Van Huffel, "Overview of total least-squares methods," *Signal Processing*, vol. 87, no. 10, pp. 2283–2302, 2007, special Section: Total Least Squares and Errors-in-Variables Modeling.
- [26] S. Derksen and H. J. Keselman, "Backward, forward and stepwise automated subset selection algorithms: Frequency of obtaining authentic and noise variables," *British journal of mathematical & statistical psychology*, vol. 45, no. 2, pp. 265–282, 1992.
- [27] S. Chen and S. A. Billings, "Representations of non-linear systems: the narmax model," *International Journal of Control*, vol. 49, no. 3, pp. 1013–1032, 1989.
- [28] G. Bontempi, "Long term time series prediction with multi-input multi-output local learning," *Proceedings of the 2nd European Symposium on Time Series Prediction (TSP), ESTSP08*, 01 2008.
- [29] N. Kanazawa, "Radial basis functions neural networks for nonlinear time series analysis and time-varying effects of supply shocks," *Journal of macroeconomics*, vol. 64, p. 103210, 2020.
- [30] R. J. Myers and S. R. Thompson, "Generalized optimal hedge ratio estimation," *American journal of agricultural economics*, vol. 71, no. 4, pp. 858–868, 1989.
- [31] W. Enders, *Applied econometric time series*, 4th ed., ser. Wiley Series in Probability and Statistics. Wiley, 2015.
- [32] H. Khosravi, "A novel structure for radial basis function networks—wrbf," *Neural processing letters*, vol. 35, no. 2, pp. 177–186, 2011.
- [33] D. E. Rumelhart, G. E. Hinton, and R. J. Williams, "Learning representations by back-propagating errors," *Nature*, vol. 323, no. 6088, pp. 533–536, 1986.
- [34] M. E. Tipping, "The relevance vector machine," in *Proceedings of the 12th International Conference on Neural Information Processing Systems*, ser. NIPS'99. Cambridge, MA, USA: MIT Press, 1999, p. 652–658.
- [35] V. N. Vapnik, *Statistical learning theory*, ser. Adaptive and learning systems for signal processing, communications, and control. New York ; Chichester: Wiley, 1998.
- [36] D. J. MacKay, "Bayesian non-linear modelling for the prediction competition," in *In ASHRAE Transactions, V.100, Pt.2*. ASHRAE, 1994, pp. 1053–1062.
- [37] R. M. Neal, *Bayesian learning for neural networks / by Radford M. Neal.*, ser. Lecture notes in statistics (Springer-Verlag) ; 118. New York: Springer, 1996.
- [38] C. E. Rasmussen and J. Quiñero-candela, "Healing the relevance vector machine through augmentation," in *In Proc. of ICML 22*, 2005.
- [39] K. Takezawa, *Introduction to nonparametric regression Kunito Takezawa.*, ser. Wiley series in probability and statistics. Hoboken, N.J: Wiley-Interscience, 2006.
- [40] N. Cristianini and J. Shawe-Taylor, *An Introduction to Support Vector Machines and Other Kernel-based Learning Methods*. Cambridge University Press, 2000.
- [41] S. E. Said and D. A. Dickey, "Testing for unit roots in autoregressive-moving average models of unknown order," *Biometrika*, vol. 71, no. 3, pp. 599–607, 12 1984.
- [42] L. Breiman, J. H. Friedman, R. A. Olshen, and C. J. Stone, *Classification and regression trees*, ser. The Wadsworth statistics/probability series. Wadsworth International Group, 1984.
- [43] D. C. Liu and J. Nocedal, "On the limited memory bfgs method for large scale optimization," *Mathematical programming*, vol. 45, no. 3, pp. 503–528, 1989.
- [44] A. Harvey, *Time series models*. Financial Times/Prentice Hall, 1993.
- [45] R. A. Meese and K. Rogoff, "Empirical exchange rate models of the seventies: Do they fit out of sample?" *Journal of international economics*, vol. 14, no. 1, pp. 3–24, 1983.
- [46] C. Engel, "Can the markov switching model forecast exchange rates?" *Journal of international economics*, vol. 36, no. 1, pp. 151–165, 1994.
- [47] L. Bachelier, "Théorie de la spéculation," *Annales Scientifiques de L'Ecole Normale Supérieure*, vol. 17, pp. 21–88, 1900.

- [48] J. Bouchaud, J. Bonart, J. Donier, and M. Gould, *Trades, Quotes and Prices: Financial Markets Under the Microscope*. Cambridge University Press, 2018.
- [49] I. Jolliffe, *Principal Component Analysis*. Berlin, Heidelberg: Springer Berlin Heidelberg, 2011, pp. 1094–1096.
- [50] T. Hastie, R. Tibshirani, and J. Friedman, *The elements of statistical learning : data mining, inference, and prediction*, ser. Springer series in statistics. Springer Verlag, 2009.
- [51] G. M. James, D. Witten, T. Hastie, and R. Tibshirani, *An introduction to statistical learning : with applications in R*, ser. Springer texts in statistics. Springer, 2013.
- [52] J. Durbin and G. S. Watson, “Testing for serial correlation in least squares regression. i,” *Biometrika*, vol. 37, pp. 409–428, 1950.
- [53] S. Gunnarsson, “Combining tracking and regularization in recursive least squares identification,” in *Proceedings of 35th IEEE Conference on Decision and Control*, vol. 3, 1996, pp. 2551–2552 vol.3.
- [54] E. Moroshko, N. Vaitis, and K. Crammer, “Second-order non-stationary online learning for regression,” *Journal of Machine Learning Research*, vol. 16, no. 43, pp. 1481–1517, 2015.
- [55] F. Pedregosa, G. Varoquaux, A. Gramfort, V. Michel, B. Thirion, O. Grisel, M. Blondel, P. Prettenhofer, R. Weiss, V. Dubourg, J. Vanderplas, A. Passos, D. Cournapeau, M. Brucher, M. Perrot, and E. Duchesnay, “Scikit-learn: Machine learning in Python,” *Journal of Machine Learning Research*, vol. 12, pp. 2825–2830, 2011.
- [56] C. Rasmussen and C. Williams, *Gaussian Processes for Machine Learning*, ser. Adaptive Computation and Machine Learning series. MIT Press, 2005.
- [57] J. H. Friedman, “Greedy function approximation: A gradient boosting machine,” *The Annals of Statistics*, vol. 29, no. 5, pp. 1189 – 1232, 2001.
- [58] W. S. Du, “Minkowski-type distance measures for generalized orthopair fuzzy sets,” *International journal of intelligent systems*, vol. 33, no. 4, pp. 802–817, 2018.
- [59] H. Munaga and V. Jarugumalli, “Performance evaluation: Ball-tree and kd-tree in the context of mst,” in *Signal Processing and Information Technology*. Berlin, Heidelberg: Springer Berlin Heidelberg, 2012, pp. 225–228.
- [60] I. Goodfellow, Y. Bengio, and A. Courville, *Deep learning*, ser. Adaptive computation and machine learning. London, England: The MIT Press, 2016.
- [61] L. Breiman, “Random forests,” *Machine learning*, vol. 45, no. 1, pp. 5–32, 2001.
- [62] A. Hoerl, “Application of ridge analysis to regression problems,” in *Chemical Engineering Progress*, 1962.
- [63] B. Schölkopf, A. J. Smola, R. C. Williamson, and P. L. Bartlett, “New support vector algorithms,” *Neural Computation*, vol. 12, no. 5, p. 1207–1245, may 2000.
- [64] B. Schölkopf, J. C. Platt, J. C. Shawe-Taylor, A. J. Smola, and R. C. Williamson, “Estimating the support of a high-dimensional distribution,” *Neural Computation*, vol. 13, no. 7, p. 1443–1471, jul 2001.
- [65] G. W. Snedecor and W. G. Cochran, “Statistical methods, eight edition,” *Iowa state University press, Ames, Iowa*, vol. 1191, 1989.
- [66] L. Wasserman, *Hypothesis Testing and p-values*. New York, NY: Springer New York, 2004, pp. 149–173.
- [67] P. Zhao, S. C. H. Hoi, J. Wang, and B. Li, “Online transfer learning,” *Artificial intelligence*, vol. 216, pp. 76–102, 2014.
- [68] B. K. Salvalaio and G. de Oliveira Ramos, “Self-adaptive appearance-based eye-tracking with online transfer learning,” in *2019 8th Brazilian Conference on Intelligent Systems (BRACIS)*. IEEE, 2019, pp. 383–388.
- [69] X. Wang, X. Wang, and Z. Zeng, “A novel weight update rule of online transfer learning,” in *2020 12th International Conference on Advanced Computational Intelligence (ICACI)*. IEEE, 2020, pp. 349–355.
- [70] J. D. Hamilton, *22 Modeling Time Series with Changes in Regime*. Princeton University Press, 2020, pp. 677–677.
- [71] A. P. Dempster, N. M. Laird, and D. B. Rubin, “Maximum likelihood from incomplete data via the em algorithm,” *Journal of the Royal Statistical Society. Series B (Methodological)*, vol. 39, pp. 1–38, 1977.



Gabriel Borrageiro is a PhD student at the University College London, in the Computer Science department and part of the Financial Computing Group. His research interests include online learning, reinforcement learning and neural networks. He obtained his executive MBA from Cass Business School, City University, London, and a computer science diploma from Damelin College, South Africa. Gabriel is employed as a quantitative researcher at BlueCrest Capital.



Nick Firoozye is currently Honorary Reader, Computational Finance, in the Computer Science department at University College London and also part of the Financial Computing Group. He obtained his PhD and MS in mathematics at New York University and a BS in mathematics at Harvey Mudd College. He also works for Exos Bank in the systematic rates trading business.



Paolo Barucca is a lecturer at University College London, Computer Science department and also part of the Financial Computing Group. He is also editor in chief of the science dissemination project, La Scienza Coatta and scientific officer of the Blockchain Education Network. Paolo received his PhD in theoretical and mathematical physics from Sapienza Università di Roma.